Published in final edited form as:
Cancer Immunol Res. 2014 July ; 2(7): 643–654. doi:10.1158/2326-6066.CIR-13-0215.

Response to BRAF inhibition in melanoma is enhanced when combined with immune checkpoint blockade

Zachary A. Cooper[1,2,*], **Vikram R. Juneja**[3,4,5,*], **Peter T. Sage**[4,5,*], **Dennie T. Frederick**[6], **Adriano Piris**[5,7], **Devarati Mitra**[5], **Jennifer A. Lo**[5], **F. Stephen Hodi**[5,8], **Gordon J. Freeman**[5,8], **Marcus W. Bosenberg**[9], **Martin McMahon**[10], **Keith T. Flaherty**[5,6], **David E. Fisher**[5,11], **Arlene H. Sharpe**[4,5,12,**], and **Jennifer A. Wargo**[1,2,**]

[1]Department of Surgical Oncology, University of Texas M.D. Anderson Cancer Center; Houston, TX USA

[2]Genomic Medicine, University of Texas M.D. Anderson Cancer Center; Houston, TX USA

[3]Harvard-MIT Division of Health Sciences and Technology, Cambridge, MA USA

[4]Department of Microbiology and Immunobiology, Boston, MA, USA

[5]Harvard Medical School, Boston, MA, USA

[6]Division of Medical Oncology, Massachusetts General Hospital; Boston, MA USA

[7]Dematopathology, Massachusetts General Hospital; Boston, MA USA

[8]Department of Medical Oncology, Dana-Farber Cancer Institute, Boston, MA USA

[9]Department of Dermatology, Yale University School of Medicine, New Haven, CT, USA

[10]Helen Diller Family Comprehensive Cancer Center, Department of Cell and Molecular Pharmacology, UCSF, San Francisco, CA, USA

[11]Dermatology, Massachusetts General Hospital; Boston, MA USA

[12]Department of Pathology, Brigham and Women's Hospital, Boston, MA, USA

Abstract

BRAF-targeted therapy results in objective responses in the majority of patients, however the responses are short-lived (~6 months). In contrast, treatment with immune checkpoint inhibitors results in a lower response rate, but the responses tend to be more durable. BRAF inhibition results in a more favorable tumor microenvironment in patients, with an increase in $CD8^+$ T-cell infiltrate and a decrease in immunosuppressive cytokines. There is also increased expression of the immunomodulatory molecule PD-L1, which may contribute to the resistance. Based on these findings, we hypothesized that BRAF-targeted therapy may synergize with the PD-1 pathway

*,**These authors contributed equally to this work

Disclosure of Potential Conflicts of Interest

A. Sharpe has licensed patents and received patent royalties from Genentech and CoStim Pharmaceuticals. G. Freeman has patents on the PD-1 pathway from Bristol-Myers-Squibb, Genentech, Merck, EMD-Serrono, Boehringer-Ingelheim, Amplimmune, and CoStim. F. S. Hodi has served as a non-paid consultant to Genentech/Roche, Merck, and Bristol-Myers Squibb and received clinical trial support from Genentech, Merck, and Bristol-Myers Squibb. K. Flaherty has served as a consultant to GlaxoSmithKline and Genentech/Roche.

blockade to enhance antitumor immunity. To test this hypothesis, we developed a BRAF(V600E)/Pten$^{-/-}$ syngeneic tumor graft immunocompetent mouse model in which BRAF inhibition leads to a significant increase in the intratumoral CD8^{+} T-cell density and cytokine production, similar to the effects of BRAF inhibition in patients. In this model CD8^{+} T cells were found to play a critical role in the therapeutic effect of BRAF inhibition. Administration of anti-PD-1 or anti-PD-L1 together with a BRAF inhibitor led to an enhanced response, significantly prolonging survival and slowing tumor growth, as well as significantly increasing the number and activity of tumor-infiltrating lymphocytes. These results demonstrate synergy between combined BRAF-targeted therapy and immune checkpoint blockade. Although clinical trials combining these two strategies are ongoing, important questions remain. Further studies using this new melanoma mouse model may provide therapeutic insights, including optimal timing and sequence of therapy.

Introduction

Targeted therapy against oncogenic mutations, such as BRAF^{V600E}, represents one of the most significant advances in the treatment of melanoma in decades. However, responses to BRAF inhibitor (BRAFi) monotherapy are not durable, with a median time to progression of less than 6 months (1–3). The combination of BRAF plus MEK (mitogen-activated or extracellular signal-regulated protein kinase) inhibition has provided incremental gains; however, the majority of patients still progress on therapy within 10 months (4). Thus, strategies to increase the durability of these responses are urgently needed.

Immunotherapy is another area of success in the treatment of melanoma. In particular, the use of immune checkpoint inhibitors has shown tremendous promise. Ipilimumab (a monoclonal antibody targeting immunomodulatory CTLA-4 receptor on T cells) was approved by the US FDA recently based on a survival benefit over standard chemotherapy in patients with metastatic melanoma (5). Additional immunomodulatory agents are in clinical trials, and have shown impressive results. These include monoclonal antibodies (mAbs) against the Programmed Death 1 (PD-1; CD279) receptor and its ligands PD-L1 (B7-H1; CD274) and PD-L2 (B7-DC; CD273) (6, 7). PD-1 is an inhibitory cell-surface receptor that can be inducibled to express by T cells, B cells, natural killer T (NK) T cells, monocytes, and dendritic cells (DCs) (8). PD-L2 is expressed mainly by DCs and macrophages, whereas PD-L1 is widely expressed by hematopoietic, non-hematopoietic, and tumor cells (8, 9). The expression of PD-L1 in tumors is inversely correlated with the survival of patients, and tumors can employ the PD-1 inhibitory pathway to evade immune eradication (10–14). Clinical trials with mAbs targeting PD-1 and PD-L1 have shown promising response rates (30–50%) with activity in melanoma and other cancers such as renal cell carcinoma and non-small cell lung cancer (6, 7). However, strategies to further improve these response rates are needed.

One exciting approach undergoing clinical investigation is the combination of BRAFi with immunotherapy to generate a sustained antitumor immune response. The rationale for this therapeutic strategy is that targeting oncogenic BRAF may make melanoma more immunogenic (15), and the eventual progression of tumors during BRAFi therapy is due to the subsequent failure of antitumor immunity (13). It is known that treatment with BRAFi

results in significantly higher expression of melanoma antigens (15, 16) and decreased expression of immunosuppressive cytokines and VEGF (16–18), all of which contribute to a tumor microenvironment that can promote antitumor immunity. Importantly, BRAFi elicits a dense $CD8^+$ T-cell infiltrate in tumors of treated melanoma patients within 10–14 days of the initiation of therapy (16, 19, 20) with increased clonality of the infiltrating T cells (21). However, a significant increase in PD-L1 expression is noted within 2 weeks of treatment with a BRAFi and the density of T-cell infiltrate in progressing lesions returns to pre-treatment levels (16). Thus, PD-1 pathway blockade has the potential to overcome BRAFi resistance and act synergistically with antitumor responses induced by BRAFi.

Several clinical trials combining BRAFi and checkpoint blockade are currently underway. Response and survival data are not mature; thus it is too early to determine if there is synergy, or if there will be added toxicity. Preliminary data from clinical trials of BRAF-targeted therapy in combination with ipilimumab indicate that there is increased toxicity, as a significant number of patients in this trial experienced hepatotoxicity (22). These early results highlight the need for additional preclinical data to support agent selection, schedule of administration, as well as to provide mechanistic insights.

In this paper, we tested the hypothesis that the addition of immune checkpoint blockade would enhance responses to BRAF-targeted therapy. First, we analyzed serial tumor biopsy samples from a patient who was treated with combined BRAF-targeted therapy and immune checkpoint blockade with anti-CTLA-4, and found increased infiltrating T cells and CD8/Treg ratio with time. Next, we built on this provocative (but anecdotal) data by testing the effects of combined BRAF-targeted therapy and immune checkpoint blockade in a novel immunocompetent and transplantable murine melanoma model that is responsive to BRAFi. We explored the effects of combined BRAFi and PD-1 or PD-L1 blockade based on our clinical findings of up-regulation of PD-L1 shortly after the initiation of BRAFi therapy (16). Similar to our findings in patient samples, we observed an increase in the intratumoral $CD8^+$ T-cell density and cytokine production in mice given BRAFi alone. Combining anti-PD-1 or anti-PD-L1 with BRAFi led to improved survival and delay in tumor growth beyond either treatment alone. Combination therapy resulted in an increase in the density of $CD8^+$ T cells in the tumor, an increased CD8/Treg ratio, and enhanced cytokine production, compared to BRAFi alone. Taken together, results from our studies indicate potent synergistic effects of combination therapy using BRAFi and PD-1 blockade. These results have important translational implications.

Materials and Methods

Clinical samples from a patient with metastatic melanoma treated with combined BRAF-targeted therapy and anti-CTLA-4

A 56-year-old male with metastatic melanoma containing a BRAF mutation (confirmed by genotyping) was enrolled in a clinical trial using combined therapy with a BRAF inhibitor (vemurafenib) and anti-CTLA4 blockade (ipilimumab) (NCT01400451). This patient was consented for tissue acquisition per our IRB-approved protocol. Serial biopsies were performed at days 0, 8, 35, 61, and 132 after the initiation of treatment. Tumors were formalin-fixed paraffin-embedded (FFPE) for immunohistochemical (IHC) analysis with a

portion processed fresh for analysis by flow cytometry (see below). All samples were analyzed via hematoxylin and eosin (H&E) staining to confirm that viable tumor was present.

Induction of melanoma tumors in Tyr:Cre(ER)T2; $Braf^{CA}$; $Pten^{lox/lox}$ mice and development of a cell line for a subcutaneous syngeneic tumor model

Tyr-Cre(ER)T2, $Braf^{CA}$, and $Pten^{lox/lox}$ animals were acquired from M. McMahon and M. Bosenberg (23) and backcrossed for over 6 generations onto the C57BL/6 genetic background (which corresponds to a >98.4% C57BL/6 congenic animal). Genotyping of each litter was performed as previously published (24). At 6–10 weeks of age mice were treated topically with 20mg/ml tamoxifen for 5 consecutive days. All studies and procedures involving animal subjects were approved by the Institutional Animal Care and Use Committees of MGH/DFCI.

To generate a tumor cell line, induced tumors were harvested and digested overnight in 10 mg/ml collagenase and 1 mg/ml hyaluronidase. Tumor cells were initially grown in RPMI media with HEPES and 20% serum, and subsequently a cell line (BP) was established and grown in DMEM media with 10% serum.

Quantitative PCR analysis of melanoma antigens in the BP cell line

The BP cell line was treated with 2μM of $BRAF^{V600E}$ inhibitor PLX4720, and RNA was extracted using the RNeasy Kit (Qiagen). Total RNA (250 ng) was used as template and Superscript VILO cDNA Synthesis Kit (Invitrogen) was used to generate cDNA. Quantitative real-time PCR was performed on an Applied Biosystems 7500 Fast Real-Time PCR System. Primer sequences used are as followed:

MITF forward: GCCTGAAACCTTGCTATGCTGGAA, MITF reverse: AAGGTACTGCTTTACCTGGTGCCT, DCT forward: AGGTACCATCTGTTGTGGCTGGAA, DCT reverse: AGTTCCGACTAATCAGCGTTGGGT, TYR forward: TGGTTCCTTTCATACCGCTC,

TYR reverse: CAGATACGACTGGCTTGTTCC, MLANA forward: TCGGCTGCTGGTACTGTAGA, MLANA reverse: GGTGATCAGGGCTCTCACAT, 18S forward: AGGTTCTGGCCAACGGTCTAG, 18S reverse: CCCTCTATGGGCAATTTT.

Ct values were normalized to untreated samples relative to 18S expression using ΔΔCt method.

Flow cytometric analysis of BP cell line

The BP cell line was treated with 20 ng/ml IFNγ in DMEM with 10% FBS for 24 hours. Cells were trypsinized to generate a single-cell suspension and stained with either anti-PD-L1 (10F.9G2; BioLegend) or MHC-I (AF6-88.5; BD Biosciences). Samples were analyzed on an LSR II (BD Biosciences) and data were analyzed with FlowJo software (TreeStar).

In vivo studies using the BP tumor cell line

8×10^5 BP cells were implanted subcutaneously (s.c.) in C57BL/6 mice on the left flank. When tumors reached ~100mm^3 mice were given *ad libitum* BRAFi (PLX4720) chow containing 200 or 417 parts per million (ppm) of PLX4720 or control chow acquired from Plexxikon Inc. For CD8 depletion, 200μg of rat anti-mouse CD8a (clone 2.43), or Rat Ig2b Kappa isotype (LTF-2) antibody was administered intraperitoneally (i.p.) 1 day before tumor implantation and every 3–4 days thereafter until time of sacrifice. For PD-1 or PD-L1 blockade experiments, 100μg of rat anti-mouse PD-1 (29F.1A12), 200μg of anti-PD-L1 (10F.9G2) (25), or isotype antibody (LTF-2) were administered i.p. on days 1, 3, and 5 following BRAFi or control chow initiation. Tumor volume was calculated as $L\times(W^2/2)$, length (L) being the longer of the two measurements.

Immunohistochemistry analyses of murine or patient tumor sections

FFPE tumor specimens were deparaffinized in xylene and hydrated in a series of ethanol dilutions. Epitope retrieval was by microwaving (5 min at 850w, 15 min at 150w) in 10 mM Tris-EDTA buffer pH 9.0. Slides were blocked 10 minutes in 3% BSA in TBST (Tris pH 7.6, 0.05% Tween-20), and rabbit polyclonal anti-CD3 antibody (Abcam ab5690, 1:100) or CD8 (Leica PA0183, RTU) in 3% BSA in TBST was applied for 1 hr at RT. HRP- labeled anti-rabbit secondary antibody (Dako EnVision, K4003, RTU) was applied for 30 minutes. Slides were developed with DAB+ (Dako K3468) for 10 min, and counterstained 1 min with hematoxylin. $CD3^+$ cell counts in 4 adjacent randomly selected intratumoral 40X fields were performed in a blinded fashion by a dermatopathologist.

Immunofluorescence analyses in murine tumor sections

Confocal microscopy was performed as described previously (26). Briefly, tissues were embedded in OCT medium (Tissue Tek) and 12 μm sections were cut using a cryostat. Sections were fixed and stained using the FoxP3 buffer set (eBiosciences) and directly conjugated antibodies. Sections were imaged on an Olympus confocal microscope with a 20x objective. For micrograph panels, single z slices were linearly contrasted and merged images were made in Adobe Photoshop. The following directly conjugated antibodies were used: anti-CD8a (53-6.7, BioLegend), anti-FoxP3 (FJK-16s, eBioscience), and anti-CD4 (RM4-5, BioLegend).

Flow cytometric analyses of tumor-infiltrating lymphocytes (TILs)

A TIL-enrichment protocol was used for both human and mouse tumors. Tumors were weighed dry, cut and placed in Collagenase Type I (400U/ml, Worthington Biochemical) and incubated on a shaker at 37°C for 30 minutes. The dissociated tumor was then filtered (70μm) to generate a single-cell suspension. A sucrose gradient (40%/70% Percoll, GE Healthcare) was used to enrich TILs from the single cell suspension. The cells were then either stimulated with PMA (50ng/ml) and ionomycin (500ng/ml) with GolgiStop (BD Biosciences) or immediately stained and subsequently analyzed by flow cytometry. The FoxP3 buffer kit (eBioscience) was used for all stains. Unstimulated human TILs were stained with the following cocktail of directly labeled antibodies: anti-CD3 (HIT3a), anti-CD4 (OKT4), anti-CD8a (HIT8a; all from Biolegend), and anti-FoxP3 (PCH101,

eBioscience). Unfractionated single-cell suspensions from mice were stained with the following cocktail of directly labeled antibodies: anti-CD31 (MEC13.3) anti-CD45 (30/F11), anti-Lyve-1 (ALY7), anti-CD105 (MJ7/8), anti-EpCAM (G8.8), and anti-PD-L1 (10F.9G2). Unstimulated mouse TILs were stained with the following directly labeled antibodies (all from Biolegend): anti-CD45.2 (104), anti-CD3e (145-2c11), anti-CD4 (RM4-5), anti-CD8a (53-6.7), anti-CD11b (M1/70), anti-Ki-67 (16A8), anti-PD-L1 (10F.9G2), anti-FoxP3 (MF-14), and anti-Granzyme B (GB11). Stimulated mouse TILs were stained with the following cocktail of directly labeled antibodies (all from Biolegend): anti-CD3e (145-2c11), anti-CD8a (53-6.7), anti-IFNγ (XMG1.2), and anti-TNFα (MP6-XT22). Isotype or Fluorescence Minus One controls were used for gating. Samples were analyzed on an LSR II (BD Biosciences) and with FlowJo software (TreeStar).

Statistics

Statistical evaluations were conducted using two-tailed Student-t test. Kaplan-Meier analysis was conducted using the Log-Rank (Mantel-Cox) test. Statistics were performed using GraphPad Prism or the R-statistical package. p values less than 0.05 were considered significant.

Results

Anti-CTLA-4 mAb synergizes with BRAF inhibition to increase the $CD8^+$/$FoxP3^+$Treg ratio within the tumor of a patient with metastatic melanoma

Given prior clinical findings showing that BRAFi is associated with improved melanoma antigen expression and an enhanced immune response in patients with metastatic melanoma (16, 19), we sought to study the effect of combined BRAF-targeted therapy and immunotherapy for the treatment of metastatic melanoma. We studied a patient with metastatic melanoma, who was participating in a clinical trial of BRAFi therapy with CTLA-4 blockade. This patient had 4 weeks of BRAFi therapy before receiving 4 courses of anti-CTLA-4 (Figure 1A). Serial tumor biopsies were stained for CD8 by IHC (Figure 1B). We found very few infiltrating $CD8^+$ T cells pre-treatment and a dense infiltrate on BRAF inhibitor therapy (as expected based on our prior findings (16)). However, within 4 weeks of BRAFi therapy the infiltrating T cells were virtually absent. One month after receiving one dose of anti-CTLA-4, the T cell infiltrate was again increased significantly and this infiltrate persisted >70 days on further anti-CTLA-4 treatment. We analyzed the TILs in tumor biopsies using flow cytometry at the same time points to assess the ratio of $CD8^+$ T cells to $CD4^+FoxP3^+$ regulatory (Treg) cells (CD8/Treg ratio) in the tumor (Figure 1C,D). These studies demonstrated an early and transient increase in the CD8/Treg ratio after the initiation of BRAF inhibitor therapy (present at 8 days but absent at 35 days after the initiation of BRAFi), mirroring our IHC findings for CD8. However, the CD8/Treg ratio increased dramatically following the administration of anti-CTLA-4 (day 61) and persisted for >70 days. These results suggest that the immune infiltrate in the setting of BRAFi is early and transient, and that immune checkpoint blockade may synergize with BRAF inhibition to heighten the immune response against melanoma.

An immunocompetent and transplantable murine melanoma model demonstrates a dose-dependent response to BRAFi

We developed a transplantable murine melanoma model in C57BL/6 mice utilizing the previously described Tyr:CreER; $Braf^{CA}$; $Pten^{lox/lox}$ mouse model (23). Melanomas in these mice form with variable latency after tamoxifen administration, making it difficult to use this model to sensitively study antitumor immunity. To circumvent this, we generated a stable cell line (BP), which was responsive to *in vitro* treatment with BRAFi (Supplementary Figure 1). Importantly, treatment of the BP line with BRAFi resulted in increased expression of known melanoma antigens including dopachrome tautomerase (TYRP2, *DCT*), tyrosinase (*TYR*), melanoma antigen recognized by T-cells (*MLANA*), and microphthalmia-associated transcription factor (*MITF*) (Figure 2A), similar to our findings in patients treated with BRAFi (16). BP tumor cells expressed the coinhibitory molecule PD-L1, and culture with IFNγ for 24 hours led to increased PD-L1 expression. IFNγ also greatly increased MHC-I expression (Figure 2B). Together, these data indicate that BP cells are likely to be recognized by $CD8^+$ T cells, while also having the potential to evade antitumor immune responses through the PD-1/PD-L1 axis.

To study the *in vivo* response of BP tumors to BRAFi, we implanted 8×10^5 BP cells (s.c.) into mice and allowed the tumors to grow to ~$100mm^3$ (Supplementary Figure 2) before administering mouse chow containing either 200 or 417 ppm of a BRAF inhibitor. BRAFi led to significantly slower tumor growth and increased survival compared to control mice (Figure 2C,D) in a dose-dependent manner. Together, these data demonstrate that the BP implanted tumor model responds to BRAF inhibition similarly to human melanoma.

BRAFi leads to increased intratumoral $CD8^+$ T-cell density and enhanced cytokine production

Based on our observations that BRAFi treatment in melanoma patients resulted in increased intratumoral $CD8^+$ T cells (16, 19, 20), we assessed the effect of BRAFi on T cells in murine BP tumors. We observed a significant dose-dependent increase in $CD3^+$ T cells 7 days following BRAFi treatment (Figure 3A and Supplementary Figure 3) composed predominantly of $CD8^+$ T cells, and some $CD4^+$ Tregs (Figure 3B). However, we did not find an increase in the expression of the nuclear proliferation marker Ki-67 in $CD8^+$ TILs in mice on BRAFi treatment (Supplementary Figure 4A).

We also evaluated effector function (cytokine production and cytolytic potential) of TILs in mice on BRAFi treatment. For cytokine analyses, we purified T cells from BP tumors and draining lymph nodes of mice 7 days after initiation of BRAFi treatment, and stimulated these cells *ex vivo* with PMA/ionomycin. Many *ex vivo* stimulated $CD8^+$ T cells from the draining lymph nodes produced TNFα but very few produced IFNγ (data not shown). Many intratumoral $CD8^+$ T cells expressed IFNγ and, to a lesser extent, TNFα (Figure 3C). Importantly, more of the intratumoral CD8+ T cells from the BRAFi-treated tumors produced both IFNγ and TNFα compared to controls (Figure 3C). Additionally, the mean fluorescence intensity (MFI) of IFNγ (in the $IFN\gamma^+$ $CD8^+$ T cells) was significantly higher in BRAFi-treated than in the control-treated cells, indicating that more IFNγ was being made on a per cell basis. To assess cytolytic potential, we measured Granzyme B production by

direct *ex vivo* analysis of intratumoral $CD8^+$ TILs. We found no difference in Granzyme B production between BRAFi and controls on day 3 of BRAFi treatment (Supplementary Figure 4B). BRAFi treatment also led to an increase in PD-L1 and PD-L2 gene expression in the tumor microenvironment (Supplementary Figure 5). Notably, PD-L1 was expressed on multiple hematopoietic and non-hematopoietic cell types in the tumor microenvironment (Supplementary Figure 6). Together, these data indicate that $CD8^+$ T cells can infiltrate melanoma tumors in the setting of BRAFi, but the tumor microenvironment is still immunosuppressive.

$CD8^+$ T cells are critical to the response to BRAF inhibition

Next, we tested whether the $CD8^+$ T cells that infiltrate tumors after BRAFi treatment were critical for the therapeutic benefit of BRAFi. We administered anti-CD8 mAb every 3–4 days (starting 1 day before BP tumor cells implantation) (Figure 4A) and initiated low dose (200 ppm) BRAFi when tumors reached $100mm^3$. $CD8^+$ T-cell depletion was maintained at days 3, 7, and 11 after BRAFi initiation in the tumor and draining lymph node as assessed by flow cytometry (Figure 4B, and data not shown). Depletion of $CD8^+$ T cells abrogated the BRAFi-induced increase in survival, with most mice dying within 20 days after tumor implantation (Figure 4C). Depletion of $CD8^+$ T cells also prevented the BRAFi-mediated decrease in tumor growth (Figure 4D). $CD8^+$ T-cell depletion similarly impeded the effects of high dose BRAFi (417ppm) on survival and tumor growth (data not shown). However, $CD8^+$ T-cell depletion did not significantly alter tumor growth in mice treated with control chow. Taken together, these data indicate that $CD8^+$ T cells are critical for the efficacy of BRAFi therapy in this mouse model of melanoma.

Blockade of the PD-1 pathway synergizes with BRAF inhibition to enhance survival and slow melanoma growth

We next tested the hypothesis that immune checkpoint blockade would synergize with BRAFi therapy to promote antitumor immunity by enhancing $CD8^+$ T-cell responses. We focused on the PD-1 pathway, given the recent clinical success of PD-1 blockade, findings of increased PD-L1 expression in tumors of patients on BRAFi, and our data showing that PD-L1 expression is increased in the BP tumors after BRAFi treatment (Supplementary Figure 5). Since tumors can be completely eradicated with high dose BRAFi but not low dose BRAFi (Figure 2C, D), we used low dose BRAFi to evaluate synergy between BRAFi and PD-1 pathway blockade. We followed a similar strategy of tumor implantation and BRAFi administration as in previous experiments (Figure 5A). We administered 3 doses of either anti-PD-1 or anti-PD-L1 (on days 1, 3, 5) after BRAFi initiation (day 0). The anti-PD-1 (29F.1A12) blocking antibody blocks the binding of PD-1 to its two ligands, PD-L1 and PD-L2. The anti-PD-L1 (10F.9G2) blocking antibody blocks interaction of PD-L1 with both of its binding partners, PD-1 and CD80 (B7-1) (27).

Treatment with anti-PD-1 alone had no effect on tumor growth or survival (Figure 5B–C). This is likely due to the large size (~1cm diameter) of the tumors before treatment with anti-PD-1, because we have seen delayed tumor growth when anti-PD-1 or anti-PD-L1 is administered earlier during tumor growth (data not shown). Notably, PD-1 pathway blockade (using either anti-PD-1 or anti-PD-L1) combined with BRAFi led to significantly

delayed tumor growth and improved survival relative to either monotherapy alone (Figure 5B–G).

PD-1 pathway blockade and BRAF inhibition synergize to enhance the number and function of tumor-infiltrating T cells

We next analyzed whether there were synergistic effects of combination therapy on TIL number and function. Combining BRAFi with either anti-PD-1 or anti-PD-L1 led to at least a 7.5-fold increase in $CD3^+$ T cells compared to any monotherapy (Figure 6A and Supplementary Figure 7). We found little to no increase in $CD3^+$ T cells in tumors treated with either anti-PD-1 or anti-PD-L1 treatment alone. Anti-PD-1 and BRAFi combination therapy led to a substantial increase in $CD8^+$ T cells in the tumor compared to BRAFi alone (Figure 6B) with no difference in $CD4^+FoxP3^-$ T cells or $CD4^+FoxP3^+$ Tregs in the tumor (Figure 6B). The CD8/Treg ratio was also increased in the combination therapy groups (Figure 6C). We also observed an increased fraction of $CD8^+$ T cells that were producing Granzyme B, as well as more polyfunctional $CD8^+$ T cells producing both IFNγ and TNFα in the mice treated with anti-PD-1 and BRAFi, but not in mice given anti-PD-L1 plus BRAFi. Together, these results suggest that the intratumoral $CD8^+$ T-cell response is synergistically enhanced by the combination therapy using BRAFi with either anti-PD-1 or anti-PD-L1.

Discussion

Two of the most significant advances in cancer treatment in decades have emerged almost concurrently: BRAF inhibitors and checkpoint blockade therapy. Support for potential synergy between BRAF-targeted therapy and immunotherapy comes from studies of serial biopsy samples of patients on targeted therapy as well as from murine studies (16, 18, 28, 29). Clinical trials combining BRAF-targeted therapy with immune checkpoint inhibitors are currently underway, although significant fundamental and translational questions remain regarding the potential mechanisms of synergy, toxicity, timing, and duration of therapy.

Here we conducted studies to understand the potential synergy between immune checkpoint blockade and BRAF-targeted therapy. We first analyzed a unique set of tumor biopsy samples from a patient receiving combined BRAF-targeted therapy and immunotherapy with vemurafenib and ipilimumab, respectively. We found that the immune response to BRAF inhibition (as assayed by T-cell infiltrate and the CD8/Treg ratio) was early and transient, but that T-cell infiltrate and an improved CD8/Treg ratio could be sustained by the addition of immune checkpoint blockade, and persist for several weeks to months. Of note, the human sample set was limited to one patient because the trial was stopped early due to toxicity (22). While this is anecdotal evidence that must be further studied in the context of clinical trials and murine models, these data suggest that the addition of immunotherapy to a backbone of targeted therapy should occur early, ideally within 2–4 weeks.

We also developed and used a novel subcutaneous implantable tumor model generated from a well-established murine model of BRAF-mutant melanoma (23). In this model we observed a dose-dependent improvement in survival after treatment with a BRAF inhibitor, which was associated with an increase in immune infiltrate and TIL function, similar to what

we observe in patients treated with BRAFi (16). The mechanism behind the increase in intratumoral T cells may reflect trafficking of T cells into the tumor (16) as well as expansion of TIL (21), which are not mutually exclusive. Data from our mouse model would suggest that proliferation of existing clones is not the dominant mechanism at an early time point, as we observe no increase in the proportion of Ki-67$^+$ CD8$^+$ TIL in BRAFi-treated mice at the two time points investigated. Of note, we previously studied this in patients and demonstrated that both mechanisms are likely at play (16, 21). In our murine model, the effects of BRAFi were attenuated with CD8$^+$ T-cell depletion suggesting a critical role for CD8$^+$ T cells in the response to BRAF inhibition. Furthermore, CD8$^+$ T-cell depletion did not affect tumor growth in mice treated with control chow, suggesting that the differences in minor histocompatibility antigens are not a major factor in the antitumor immunity in these mice.

In addition to an enhanced T-cell infiltrate, we found that BRAFi treatment led to the upregulation of PD-L1 and an increase in IFNγ–expressing TILs. This is consistent with our published findings from tumor biopsies of patients with melanoma on BRAFi therapy, demonstrating an increase in PD-L1 expression within 2 weeks of the initiation of therapy (16). Recent literature suggests that this is related to IFNγ production by TIL (30) or stromal fibroblasts (31). Human studies have also shown that PD-L1 expression co-localizes with infiltrating T cells (32). In our murine model, PD-L1 is expressed on a wide variety of cells in the tumor microenvironment, including CTLs, myeloid cells, epithelial cells, endothelial cells, lymphatic endothelial cells, and tumor cells in the setting of BRAFi. Together these data, coupled with a better toxicity profile of PD-1 pathway blockade in patients (5–7), gave impetus to our study of the effects of combined BRAF-targeted therapy with PD-1 or PD-L1 blockade in the BP tumor model.

We studied the combined regimen of BRAF-targeted therapy and anti-PD-1 or anti-PD-L1 blockade in our murine model, and observed enhanced survival and delayed tumor outgrowth compared to BRAFi or PD-1 pathway blockade alone. Delayed tumor growth was accompanied by an increase in CD8$^+$ T-cell density and function in these groups. Specifically, CD8$^+$ TILs expressed more IFNγ, TNFα, and Granzyme B in mice given combined BRAFi and PD-1 blockade. This is in contrast to findings in mice receiving BRAF inhibitor monotherapy demonstrating increased expression of IFNγ and TNFα in TILs, but not Granzyme B. These data suggest that BRAF inhibition alone results in an increase in T-cell infiltration and cytokine production, but these T cells are not completely functional. Thus, BRAFi and PD-1 pathway blockade synergize to increase CD8$^+$ TIL cell density and function, indicating that the PD-1 pathway plays a significant role in immune modulation in our BP tumor model.

Of note, we found a similar increase in TIL after combined BRAFi plus anti-PD-L1 administration, but did not observe increased T-cell functionality based on cytokines or Granzyme B. There are several possible reasons for this difference. First, there may be differences in the kinetics of the T-cell response to anti-PD-1 versus anti-PD-L1 after BRAFi treatment. In addition, the expression of PD-L2 as well as PD-L1 in the tumor microenvironment may explain these differences. MAbs targeting PD-1 and PD-L1 may have different functional effects as they block distinct receptor-ligand interactions. PD-1

binds to PD-L1 and PD-L2 whereas PD-L1 binds to PD-1 and B7-1 (CD80) (27, 33). Anti-PD-1 blocks PD-1 interaction with PD-L1 or PD-L2, but does not perturb the PD-L1/B7-1 pathway. The anti-PD-L1 used here is a dual blocker, blocking PD-L1 interactions with PD-1 and B7-1, but leaving the PD-1/PD-L2 interactions intact. Thus, the expression of PD-L2 in our mouse melanoma model may underlie the diverse effects when BRAFi is combined with anti-PD-L1 vs. anti-PD-1. The differential effects of anti-PD-L1 and anti-PD-1 Abs as well as differences in PD-L1 and PD-L2 expression have clinical implications and may explain the subtle variations in the clinical effects observed when blocking either PD-1 or PD-L1 alone (6, 7).

Further work is needed to understand how anti-PD-1 and anti-PD-L1 exert their antitumor effects. PD-1 is upregulated upon activation of T cells in peripheral lymphoid organs, on activated T cells in the tumor, as well as dysfunctional (termed “exhausted” T cells) in the tumor microenvironment (34, 35). Anti-PD-1 likely affects the activation and function of T cells both in the tumor and in secondary lymphoid organs, and rescues exhausted T cells in the tumor (7, 36, 37). Furthermore, PD-1 blockade also may have functional consequences on other PD-1-expressing cell types (26). Studies of the effects of PD-1 blockade on the function of PD-1^+ NK cells and macrophages in the tumor are ongoing (38, 39). Similarly, PD-L1 is expressed by multiple cell types, both in and outside of the tumor (8). PD-L1 expression in lymphoid organs may suppress the initial activation of T cells and/or enhance the induction of Tregs (40). Within the tumor, PD-L1 can be expressed by both tumor and non-tumor cells, both of which have the potential to suppress antitumor immunity (41, 42). Our studies in the LCMV chronic infection model indicate that PD-L1 on hematopoietic and non-hematopoietic cells can both contribute to T-cell exhaustion (43). Clinical data indicate that PD-1 pathway blockade can be successful even when tumors do not express PD-L1, suggesting that PD-L1 expression on tumor cells is not required for response (44).

It is important to note that we initiated treatment with BRAFi when tumors were large (~100mm^3 in volume) and we then administered PD-1 pathway blocking antibodies only after BRAFi initiation. This approach is clinically relevant to patients with a high metastatic burden, as response rates to immune checkpoint blockade are not universal and may be delayed. Although we did not observe a significant difference in survival or growth after anti-PD-1 or anti-PD-L1 monotherapy when administered at this late time point, we found a significant difference in survival when PD-1 or PD-L1 blockade monotherapy was given to mice with smaller tumors (data not shown). Thus, this subcutaneous melanoma model could be used to model and study multiple clinically relevant scenarios.

Our results are consistent with several published studies that demonstrate synergy of BRAF-directed therapy with other immunotherapies in murine models (18, 28, 29). Studies using adoptive T-cell transfer, anti-CCL2 or anti-CD137 (18, 28, 29) have demonstrated synergy between BRAF-targeted therapy and immunotherapy with enhanced survival and T-cell function. Conversely, one study showed no synergy when BRAF-targeted therapy was combined with immune checkpoint blockade (45). This study used a similar BRAF/Pten model with induced primary tumors as opposed to subcutaneous tumors. BRAFi treatment of induced primary tumors resulted in a decrease in immune infiltrate, which is not consistent with what we observe in metastatic melanoma tumors from patients treated with

BRAFi (16, 19). In this primary tumor model, the addition of CTLA-4 blockade, either with or without BRAFi, did not improve survival or delay tumor growth (45). Further studies are needed to determine if this lack of synergy reflects the different biology in the primary tumor model.

In conclusion, these studies provide evidence that immune checkpoint blockade using anti-PD-1 or anti-PD-L1 synergizes with BRAF-targeted therapy to improve responses in a BRAF-mutant model of melanoma. This novel mouse melanoma model provides a new means to address important translational questions about combining BRAFi and immunotherapy and to complement correlative studies on clinical trials combining immune checkpoint inhibitors with BRAFi.

Supplementary Material

Refer to Web version on PubMed Central for supplementary material.

Acknowledgments

Grant support:

JAW acknowledges NIH grants 1K08CA160692-01A1 and P30CA016672, and from philanthropic support of several families whose lives have been affected by melanoma. JAW, AHS, and GJF acknowledge support from U54CA163125. AHS and GJF acknowledge P01AI056299. AHS and GJF also acknowledge support from DF HCC Kidney Cancer SPORE P50CA101942. DEF acknowledges support from NIH grant P01 CA163222 and a grant from the Dr. Miriam and Sheldon G. Adelson Medical Research Foundation. PTS acknowledges support from NIH grant (5T32HL007627-28). VRJ acknowledges support from the Department of Defense and from a National Science Foundation Graduate Fellowship.

References

1. Flaherty KT, Puzanov I, Kim KB, Ribas A, McArthur GA, Sosman JA, et al. Inhibition of mutated, activated BRAF in metastatic melanoma. The New England journal of medicine. 2010; 363:809–19. [PubMed: 20818844]
2. Sosman JA, Kim KB, Schuchter L, Gonzalez R, Pavlick AC, Weber JS, et al. Survival in BRAF V600-mutant advanced melanoma treated with vemurafenib. The New England journal of medicine. 2012; 366:707–14. [PubMed: 22356324]
3. Chapman PB, Hauschild A, Robert C, Haanen JB, Ascierto P, Larkin J, et al. Improved survival with vemurafenib in melanoma with BRAF V600E mutation. The New England journal of medicine. 2011; 364:2507–16. [PubMed: 21639808]
4. Flaherty KT, Infante JR, Daud A, Gonzalez R, Kefford RF, Sosman J, et al. Combined BRAF and MEK Inhibition in Melanoma with BRAF V600 Mutations. The New England journal of medicine. 2012; 367:1694–703. [PubMed: 23020132]
5. Hodi FS, O'Day SJ, McDermott DF, Weber RW, Sosman JA, Haanen JB, et al. Improved survival with ipilimumab in patients with metastatic melanoma. The New England journal of medicine. 2010; 363:711–23. [PubMed: 20525992]
6. Brahmer JR, Tykodi SS, Chow LQ, Hwu WJ, Topalian SL, Hwu P, et al. Safety and activity of anti-PD-L1 antibody in patients with advanced cancer. The New England journal of medicine. 2012; 366:2455–65. [PubMed: 22658128]
7. Topalian SL, Hodi FS, Brahmer JR, Gettinger SN, Smith DC, McDermott DF, et al. Safety, activity, and immune correlates of anti-PD-1 antibody in cancer. The New England journal of medicine. 2012; 366:2443–54. [PubMed: 22658127]
8. Keir ME, Butte MJ, Freeman GJ, Sharpe AH. PD-1 and its ligands in tolerance and immunity. Annual review of immunology. 2008; 26:677–704.

9. Keir ME, Liang SC, Guleria I, Latchman YE, Qipo A, Albacker LA, et al. Tissue expression of PD-L1 mediates peripheral T cell tolerance. The Journal of experimental medicine. 2006; 203:883–95. [PubMed: 16606670]
10. Ohigashi Y, Sho M, Yamada Y, Tsurui Y, Hamada K, Ikeda N, et al. Clinical significance of programmed death-1 ligand-1 and programmed death-1 ligand-2 expression in human esophageal cancer. Clinical cancer research : an official journal of the American Association for Cancer Research. 2005; 11:2947–53. [PubMed: 15837746]
11. Konishi J, Yamazaki K, Azuma M, Kinoshita I, Dosaka-Akita H, Nishimura M. B7-H1 expression on non-small cell lung cancer cells and its relationship with tumor-infiltrating lymphocytes and their PD-1 expression. Clinical cancer research : an official journal of the American Association for Cancer Research. 2004; 10:5094–100. [PubMed: 15297412]
12. Thompson RH, Kuntz SM, Leibovich BC, Dong H, Lohse CM, Webster WS, et al. Tumor B7-H1 is associated with poor prognosis in renal cell carcinoma patients with long-term follow-up. Cancer research. 2006; 66:3381–5. [PubMed: 16585157]
13. Thompson RH, Gillett MD, Cheville JC, Lohse CM, Dong H, Webster WS, et al. Costimulatory B7-H1 in renal cell carcinoma patients: Indicator of tumor aggressiveness and potential therapeutic target. Proceedings of the National Academy of Sciences of the United States of America. 2004; 101:17174–9. [PubMed: 15569934]
14. Blank C, Brown I, Marks R, Nishimura H, Honjo T, Gajewski TF. Absence of programmed death receptor 1 alters thymic development and enhances generation of CD4/CD8 double-negative TCR-transgenic T cells. J Immunol. 2003; 171:4574–81. [PubMed: 14568931]
15. Boni A, Cogdill AP, Dang P, Udayakumar D, Njauw CN, Sloss CM, et al. Selective BRAFV600E inhibition enhances T-cell recognition of melanoma without affecting lymphocyte function. Cancer research. 2010; 70:5213–9. [PubMed: 20551059]
16. Frederick DT, Piris A, Cogdill AP, Cooper ZA, Lezcano C, Ferrone CR, et al. BRAF inhibition is associated with enhanced melanoma antigen expression and a more favorable tumor microenvironment in patients with metastatic melanoma. Clinical cancer research : an official journal of the American Association for Cancer Research. 2013; 19:1225–31. [PubMed: 23307859]
17. Khalili JS, Liu S, Rodriguez-Cruz TG, Whittington M, Wardell S, Liu C, et al. Oncogenic BRAF(V600E) Promotes Stromal Cell-Mediated Immunosuppression Via Induction of Interleukin-1 in Melanoma. Clinical cancer research : an official journal of the American Association for Cancer Research. 2012; 18:5329–40. [PubMed: 22850568]
18. Liu C, Peng W, Xu C, Lou Y, Zhang M, Wargo JA, et al. BRAF inhibition increases tumor infiltration by T cells and enhances the antitumor activity of adoptive immunotherapy in mice. Clinical cancer research : an official journal of the American Association for Cancer Research. 2013; 19:393–403. [PubMed: 23204132]
19. Wilmott JS, Long GV, Howle JR, Haydu LE, Sharma RN, Thompson JF, et al. Selective BRAF inhibitors induce marked T-cell infiltration into human metastatic melanoma. Clinical cancer research : an official journal of the American Association for Cancer Research. 2012; 18:1386–94. [PubMed: 22156613]
20. Wargo, J.; Cogdill, A.; Dang, P.; Gupta, R.; Piris, A.; Boni, A., et al. Treatment with a selective inhibitor of BRAFV600E increases melanocyte antigen expression and CD8 T cell infiltrate in tumors of patients with metastatic melanoma. American Association for Cancer Research 102nd Annual Meeting; 2011; Orlando, Fl. 2011. p. 232
21. Cooper ZA, Frederick DT, Juneja VR, Sullivan RJ, Lawrence DP, Piris A, et al. BRAF inhibition is associated with increased clonality in tumor-infiltrating lymphocytes. Oncoimmunology. 2013; 2:e26615. [PubMed: 24251082]
22. Ribas A, Hodi FS, Callahan M, Konto C, Wolchok J. Hepatotoxicity with combination of vemurafenib and ipilimumab. The New England journal of medicine. 2013; 368:1365–6. [PubMed: 23550685]
23. Dankort D, Curley DP, Cartlidge RA, Nelson B, Karnezis AN, Damsky WE Jr, et al. Braf(V600E) cooperates with Pten loss to induce metastatic melanoma. Nat Genet. 2009; 41:544–52. [PubMed: 19282848]

24. Mitra D, Luo X, Morgan A, Wang J, Hoang MP, Lo J, et al. An ultraviolet-radiation-independent pathway to melanoma carcinogenesis in the red hair/fair skin background. Nature. 2012; 491:449–53. [PubMed: 23123854]
25. Rodig N, Ryan T, Allen JA, Pang H, Grabie N, Chernova T, et al. Endothelial expression of PD-L1 and PD-L2 down-regulates CD8+ T cell activation and cytolysis. European journal of immunology. 2003; 33:3117–26. [PubMed: 14579280]
26. Sage PT, Francisco LM, Carman CV, Sharpe AH. The receptor PD-1 controls follicular regulatory T cells in the lymph nodes and blood. Nature immunology. 2013; 14:152–61. [PubMed: 23242415]
27. Butte MJ, Keir ME, Phamduy TB, Sharpe AH, Freeman GJ. Programmed death-1 ligand 1 interacts specifically with the B7-1 costimulatory molecule to inhibit T cell responses. Immunity. 2007; 27:111–22. [PubMed: 17629517]
28. Knight DA, Ngiow SF, Li M, Parmenter T, Mok S, Cass A, et al. Host immunity contributes to the anti-melanoma activity of BRAF inhibitors. The Journal of clinical investigation. 2013; 123:1371–81. [PubMed: 23454771]
29. Koya RC, Mok S, Otte N, Blacketor KJ, Comin-Anduix B, Tumeh PC, et al. BRAF inhibitor vemurafenib improves the antitumor activity of adoptive cell immunotherapy. Cancer research. 2012; 72:3928–37. [PubMed: 22693252]
30. Spranger S, Spaapen RM, Zha Y, Williams J, Meng Y, Ha TT, et al. Up-regulation of PD-L1, IDO, and T(regs) in the melanoma tumor microenvironment is driven by CD8(+) T cells. Science translational medicine. 2013; 5:200ra116.
31. Frederick, DT.; Ahmed, Z.; Cooper, ZA.; Lizee, G.; Hwu, P.; Ferrone, CR., et al. Stromal fibroblasts contribute to the up-regulation of PD-L1 in melanoma after BRAF inhibition. Society For Melanoma Research 2013 International Congress; 2013; Philadelphia, PA. 2013. p. 950-1.
32. Taube JM, Anders RA, Young GD, Xu H, Sharma R, McMiller TL, et al. Colocalization of inflammatory response with B7-h1 expression in human melanocytic lesions supports an adaptive resistance mechanism of immune escape. Science translational medicine. 2012; 4:127ra37.
33. Paterson AM, Brown KE, Keir ME, Vanguri VK, Riella LV, Chandraker A, et al. The programmed death-1 ligand 1:B7-1 pathway restrains diabetogenic effector T cells in vivo. J Immunol. 2011; 187:1097–105. [PubMed: 21697456]
34. Fourcade J, Sun Z, Benallaoua M, Guillaume P, Luescher IF, Sander C, et al. Upregulation of Tim-3 and PD-1 expression is associated with tumor antigen-specific CD8+ T cell dysfunction in melanoma patients. The Journal of experimental medicine. 2010; 207:2175–86. [PubMed: 20819923]
35. Chapon M, Randriamampita C, Maubec E, Badoual C, Fouquet S, Wang SF, et al. Progressive upregulation of PD-1 in primary and metastatic melanomas associated with blunted TCR signaling in infiltrating T lymphocytes. The Journal of investigative dermatology. 2011; 131:1300–7. [PubMed: 21346771]
36. Zippelius A, Batard P, Rubio-Godoy V, Bioley G, Lienard D, Lejeune F, et al. Effector function of human tumor-specific CD8 T cells in melanoma lesions: a state of local functional tolerance. Cancer research. 2004; 64:2865–73. [PubMed: 15087405]
37. Hamid O, Robert C, Daud A, Hodi FS, Hwu WJ, Kefford R, et al. Safety and tumor responses with lambrolizumab (anti-PD-1) in melanoma. The New England journal of medicine. 2013; 369:134–44. [PubMed: 23724846]
38. Benson DM Jr, Bakan CE, Mishra A, Hofmeister CC, Efebera Y, Becknell B, et al. The PD-1/PD-L1 axis modulates the natural killer cell versus multiple myeloma effect: a therapeutic target for CT-011, a novel monoclonal anti-PD-1 antibody. Blood. 2010; 116:2286–94. [PubMed: 20460501]
39. Duraiswamy J, Freeman GJ, Coukos G. Therapeutic PD-1 Pathway Blockade Augments with Other Modalities of Immunotherapy T-Cell Function to Prevent Immune Decline in Ovarian Cancer. Cancer research. 2013
40. Francisco LM, Salinas VH, Brown KE, Vanguri VK, Freeman GJ, Kuchroo VK, et al. PD-L1 regulates the development, maintenance, and function of induced regulatory T cells. The Journal of experimental medicine. 2009; 206:3015–29. [PubMed: 20008522]

41. Curiel TJ, Wei S, Dong H, Alvarez X, Cheng P, Mottram P, et al. Blockade of B7-H1 improves myeloid dendritic cell-mediated antitumor immunity. Nature medicine. 2003; 9:562–7.

42. Blank C, Kuball J, Voelkl S, Wiendl H, Becker B, Walter B, et al. Blockade of PD-L1 (B7-H1) augments human tumor-specific T cell responses in vitro. International journal of cancer Journal international du cancer. 2006; 119:317–27. [PubMed: 16482562]

43. Mueller SN, Vanguri VK, Ha SJ, West EE, Keir ME, Glickman JN, et al. PD-L1 has distinct functions in hematopoietic and nonhematopoietic cells in regulating T cell responses during chronic infection in mice. The Journal of clinical investigation. 2010; 120:2508–15. [PubMed: 20551512]

44. Herbst, R.; Gordon, M.; Fine, G.; Sosman, J.; Soria, J.; Hamid, O., et al. A study of MPDL3280A, an engineered PD-L1 antibody in patients with locally advanced or metastatic tumors. Journal of Clinical Oncology (Meeting Abstracts); 2013 ASCO Annual Meeting; 2013; Chicago, Il. 2013.

45. Hooijkaas A, Gadiot J, Morrow M, Stewart R, Schumacher T, Blank CU. Selective BRAF inhibition decreases tumor-resident lymphocyte frequencies in a mouse model of human melanoma. Oncoimmunology. 2012; 1:609–17. [PubMed: 22934253]

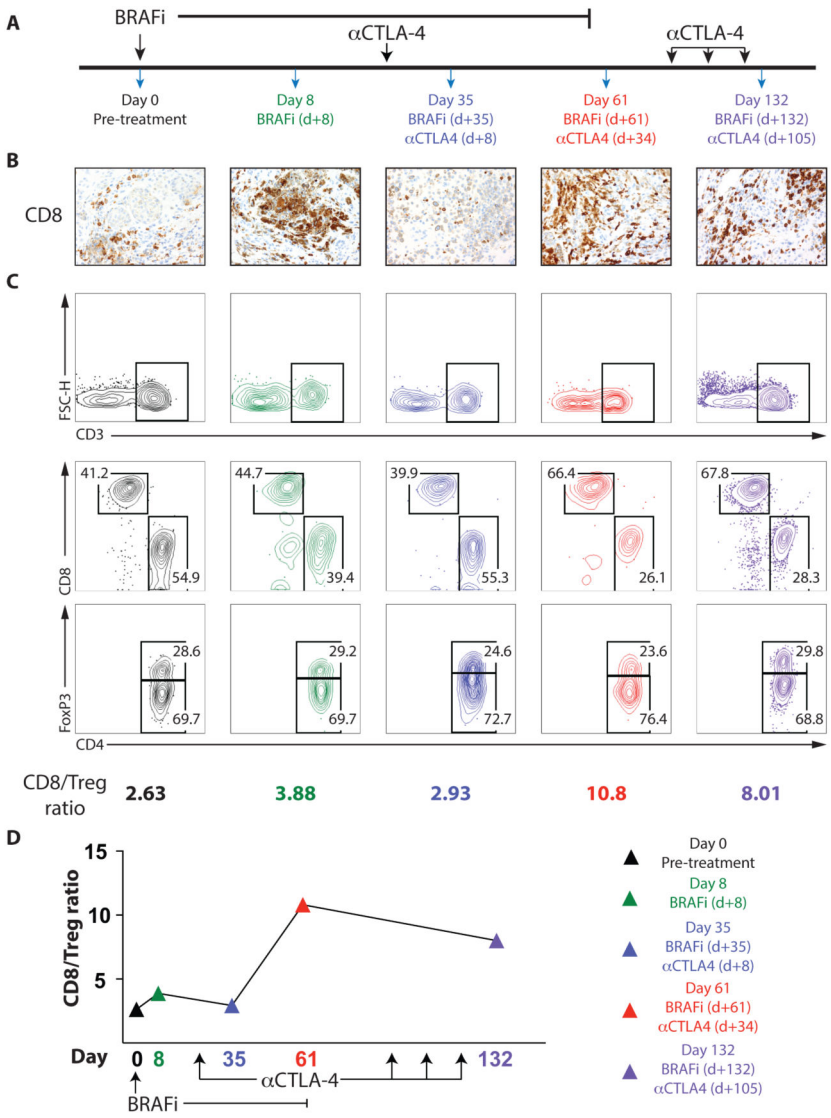

Figure 1. Combined BRAF inhibitor and anti-CTLA-4 administration leads to prolonged antitumor immunity in a patient with metastatic melanoma

A patient with metastatic melanoma was treated with combined BRAF-targeted therapy plus CTLA-4 blockade. A, Timeline showing treatment schedule and biopsies B, $CD8^+$ T-cell infiltrate was determined by IHC (40x magnification). C and D, Immune cells isolated from tumors were analyzed by flow cytometry. (C, Top) $CD3^+$ lymphocytes. FSC-H, forward scatter height. (C, Middle) Populations of $CD4^+$ and $CD8^+$ lymphocytes pregated on $CD3^+$ cells. (C, Bottom) Percentage of $CD4^+FoxP3^+$ T regulatory cells (Treg) and $CD4^+FoxP3^-$ non-Tregs, pregated on $CD3^+CD4^+$ T cells. The ratio of $CD8^+$ T cells to $CD4^+FoxP3^+$ Treg cells is shown (C) and plotted versus time (D).

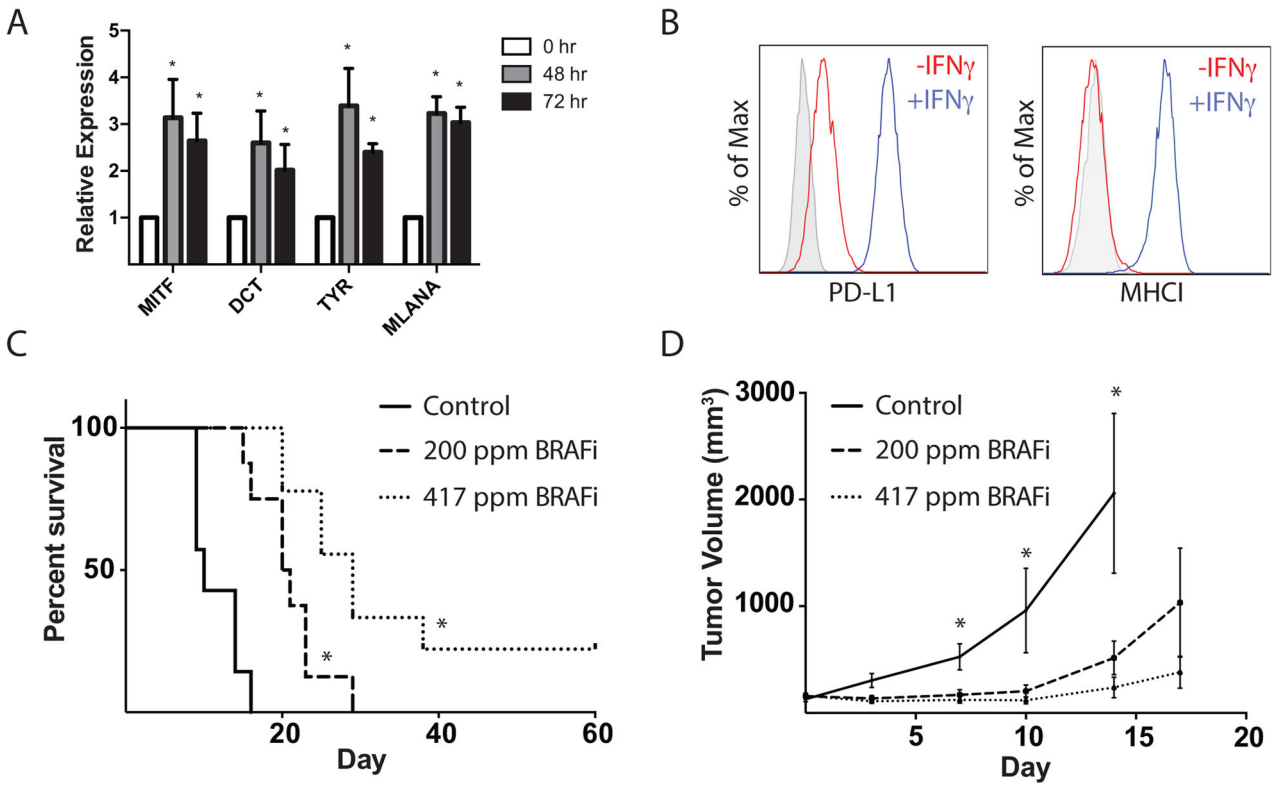

Figure 2. BRAF inhibition results in a dose-dependent increase in survival and a slowing of tumor growth in a syngeneic implantable tumor model

A, Comparison of expression of *DCT*, *TYR*, *MLANA* and *MITF* melanoma antigen mRNA (relative to 18S RNA) in the $BRAF^{V600E}/Pten^{-/-}$, or BP, cell line that was cultured with 2μM of BRAFi for 0, 48 or 72hrs. B, Comparison of surface expression of PD-L1 and MHC class I (MHCI) on BP cells cultured with (red) or without (blue) IFNγ for 24 hours. Gray indicates unstained cells. C, 8×10^5 BP cells were implanted subcutaneously in C57BL/6. When tumors reached ~$100mm^3$, BRAFi was administered at 200 or 417 ppm (day 0). Survival is shown in a Kaplan-Meier plot. Mice were sacrificed when tumors reached a maximum diameter of 2cm or had ulceration (n≥7). *, $p< 0.05$ comparing BRAFi-treated mice to control mice. D, Tumor growth curves for experiments as in (C). Tumor volumes were measured every 3–4 days (n≥10). *, $p< 0.05$ comparing BRAFi-treated mice to control mice.

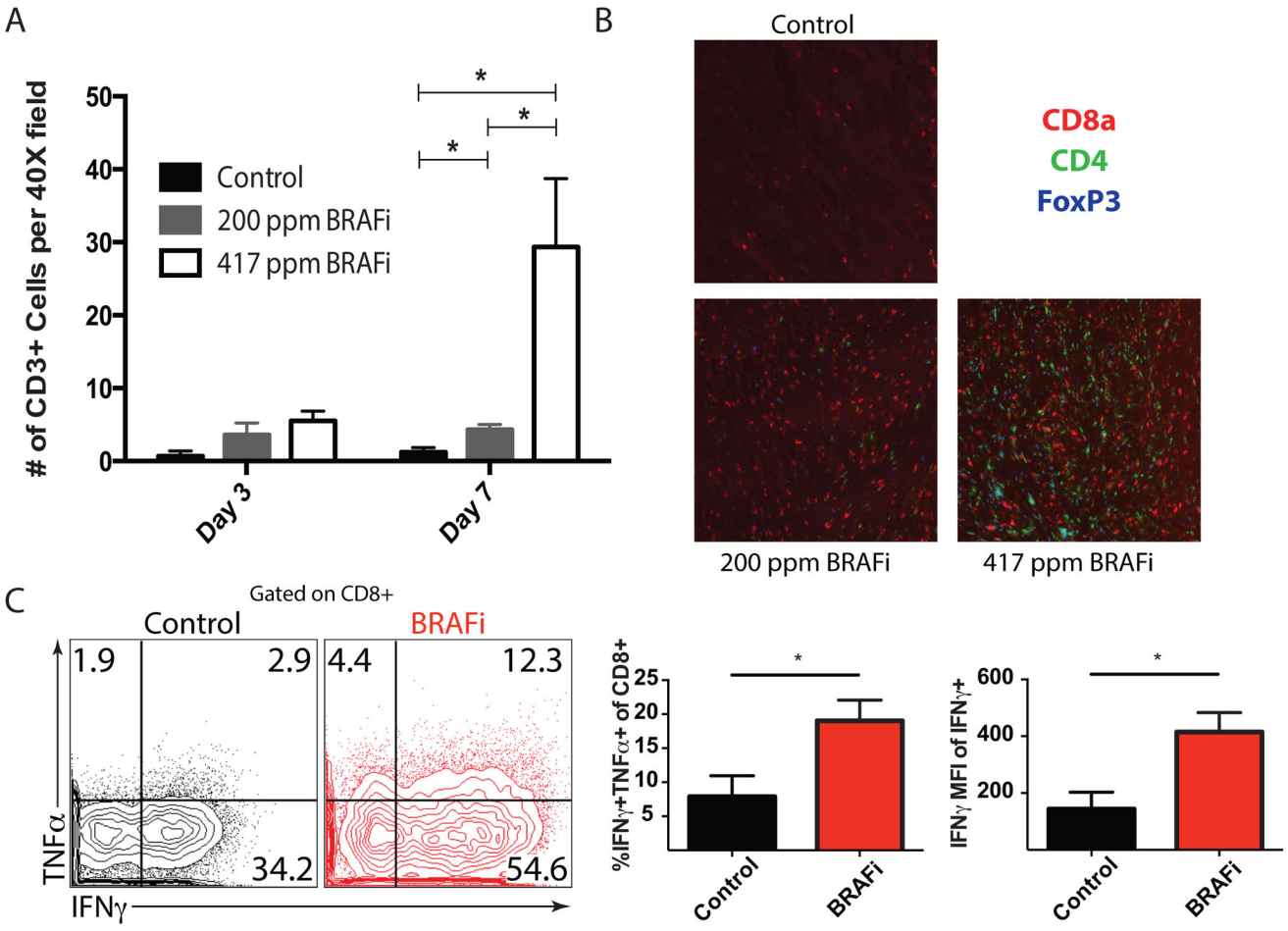

Figure 3. BRAF inhibition is associated with an increase in cytokine production and density of tumor-infiltrating T cells

A, Subcutaneously implanted BP tumors were harvested 3 or 7 days after BRAFi initiation. CD3 expression was assayed via IHC in 3 randomly selected intratumoral 40X fields by a dermatopathologist. n=3, $p<0.05$. B, OCT-embedded BP tumors (harvested 7 days after BRAFi initiation) were stained for CD8a, CD4, and FoxP3. Representative fields are shown (200X magnification). C, Expression of IFNγ and TNFα by intratumoral immune-cell infiltrates stimulated *ex vivo* with PMA/ionomycin, was assayed via flow cytometry. Plots are pre-gated on $CD3^+CD8^+$ T cells (left). Average percentage of $IFN\gamma^+TNF\alpha^+$ T cells (of $CD3^+CD8^+$ cells) and mean fluorescence intensity (MFI) of IFNγ on $IFN\gamma^+CD8^+$ T cells are shown (n=5 per group).

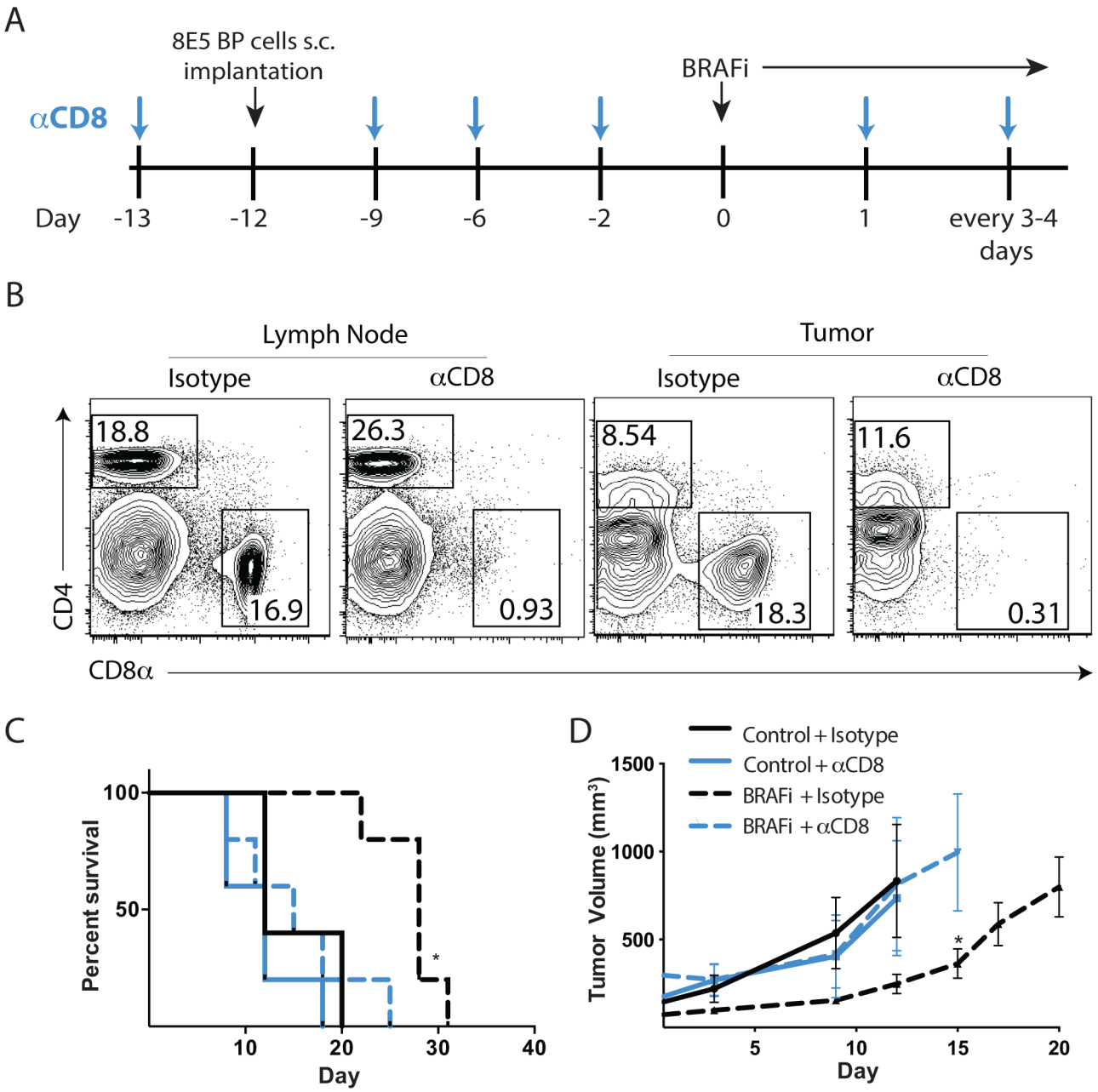

Figure 4. CD8 T cells play a critical role in responses of tumor-infiltrating lymphocytes due to BRAF inhibition

A, Schema for CD8 T cell-depletion in BP tumors. 8×10^5 BP cells were s.c. injected into C57BL/6 mice and BRAFi administration (200 ppm) was initiated at day 0. 200μg of rat anti-mouse CD8, or isotype antibody was administered i.p. 1 day before tumor implantation and every 3–4 days thereafter. B, Analysis of $CD4^+$ and $CD8^+$ T cells in the draining lymph node and tumor were evaluated on days 3, 7 and 11 after the initiation of BRAFi for CD8 T cell depletion by flow cytometry using a different anti-CD8 clone. Representative plots at day 3 are shown. C, Effects of CD8 depletion on survival of mice given BP tumor with or without BRAFi therapy displayed in a Kaplan-Meier plot. *, $p< 0.05$ comparing BRAFi

treated mice to control mice. D, Tumor volumes from experiments as in (C) measured every 3–4 days. *, $p < 0.05$ comparing BRAFi + isotype treated mice to BRAFi + anti-CD8 mAb-treated mice. Representative of 3 experiments.

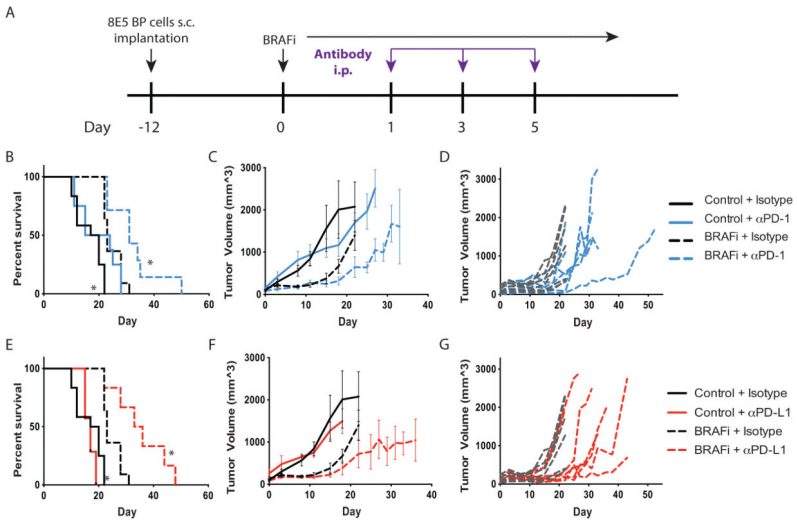

Figure 5. PD-1 or PD-L1 blockade synergizes with BRAF inhibition to slow tumor growth and increase survival

A, Schema for combination treatment using PD-1/PD-L1 blockade and BRAFi after BP cell implantation. 8×10^5 BP cells were given to C57BL/6 mice s.c., and BRAFi (200 ppm) was initiated at day 0. 100μg of anti-PD-1 (29F.1A12), 200μg anti-PD-L1 (10F.9G2), or isotype antibody was administered i.p. at days 1, 3, and 5. B–D, Effects of combined BRAFi and anti-PD-1 on the survival and tumor volumes in mice given BP tumor cells. Kaplan-Meier plot showing survival after BRAFi and anti-PD-1 combined treatment averaged for all mice in each treatment group (B). Tumor volumes (measured every 3–4 days) are averaged (C) and shown for individual mice for BRAFi plus isotype control versus BRAFi + anti-PD-1 (D). E–G, Effects of combined BRAFi and anti-PD-L1 on the survival of mice given BP tumor cells. Kaplan-Meier plot showing survival after BRAFi and anti-PD-L1 combined treatment averaged for all mice in each treatment group (E). Tumor volumes (measured every 3–4 days) are averaged (F) and shown for individual mice for BRAFi + isotype control versus BRAFi plus anti-PD-L1 (G). For the Kaplan-Meier plot, control + isotype (n=12), BRAFi + isotype (n=11), control + anti-PD-1 (n=8) or anti-PD-L1 (n=7) or BRAFi + anti-PD-1 (n=7) or anti-PD-L1 (n=6). *, $p< 0.05$ compared to BRAFi + isotype mice. Tumor volumes are representative of 3 experiments (n>6).

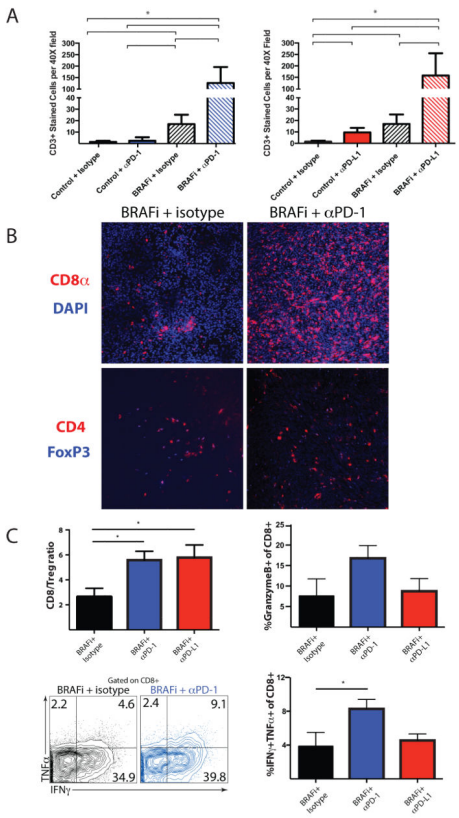

Figure 6. PD-1 pathway blockade and BRAF inhibition synergize to enhance number and function of tumor-infiltrating T cells

Experiment was performed as in Figure 5. A, $CD3^+$ T cells were assayed via IHC in tumors of mice given BRAFi plus anti-PD-1, anti-PD-L1 or control mAb. $n \geq 3$, $p < 0.05$. B, $CD4^+$, $CD8^+$ and $FoxP3^+$ expression was assayed via immunofluorescence (IF) within tumors of mice given BRAFi plus anti-PD-1 or isotype control mAb. Representative sections are shown (200X magnification). C, Immune infiltrates in tumors harvested 14 days after BRAFi initiation were characterized by flow cytometry. The ratios of $CD8^+$ T cells to Tregs ($CD4^+FoxP3^+$) are shown, as are percentage of $CD8^+$ T cells that are positive for Granzyme B or for IFNγ and TNFα. Representative flow plots for IFNγ and TNFα expression in $CD8^+$ T cells are shown.